

Continuous cell sorting in a flow based on single cell resonance Raman spectra

David McIlvenna¹, Wei E. Huang², Paul Davison³, Andrew Glidle¹, Jon Cooper¹, and Huabing Yin^{1*}

Supplementary Information:

Supplementary Video 1. Automatically switching individual beads to alternate outlets every 0.5 seconds (i.e 2 Hz).

Supplementary Video 2. Continuous delivery of a stream of individual cells to the detection point (i.e. the green dot).

Supplementary Video 3. Automated, Raman activated single cell sorting. Single cell Raman spectra are acquired continuously and analysed on-the-fly to classify cell type. Classification of each spectrum is updated *in situ* as “nothing”, “C12” or “C13”, as shown on the panel. When a target cell (e.g. ¹³C cell) is identified, “trigger”, as indicated by the “on” green light on the panel, will be sent to the pump to change the setting of the output pressures.

1. Effect of mechanical disturbances at low flow rates.

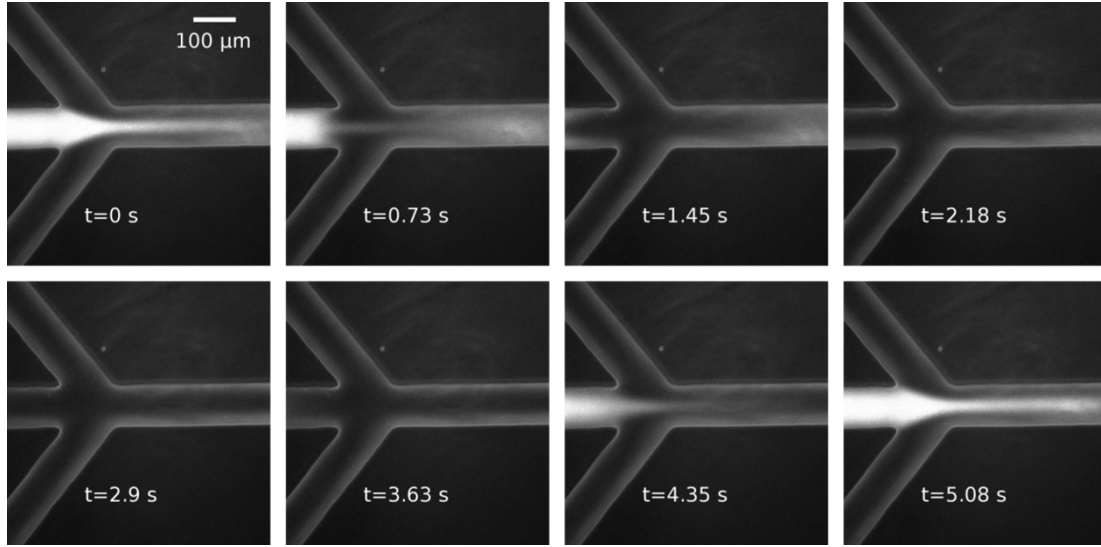


Figure S1. Timelapse fluorescence images of fluorescein solution after valve closing at one of the two outlets. The fluorescein flow is of $0.275 \mu\text{L.h}^{-1}$ fluorescein and the buffer flows are of $1.25 \mu\text{L.h}^{-1}$. The displacement of liquid caused by the valves closing interrupts the input flow from the sample channel. This takes approximately 4 seconds to be re-established due to the low input flow rate to the sample channel.

2. The Poiseuille effect on microflow

The flow generated by an applied pressure is not uniform across the entire cross-section of a channel. Flow rates nearer the centre of a channel are faster than those at the boundaries. This effect is described by Equation S1 [1] for a channel as illustrated in Figure S2.

$$u(y, z) = \frac{16a^2}{\mu\pi^3} \left(-\frac{d\bar{p}}{dx} \right) \sum_{i=1,3,5,\dots}^{\infty} (-1)^{\frac{i-1}{2}} \left[1 - \frac{\frac{\cosh i\pi z}{2a}}{\frac{\cosh i\pi b}{2a}} \right] \frac{\cos \frac{i\pi y}{2a}}{i^3} \quad \text{Equation S1}$$

where $-a \leq y \leq a$, $-b \leq z \leq b$,

$a = w/2$, i.e. half of the channel width,

$b = h/2$, i.e. half of the channel height, and

μ is the fluid density.

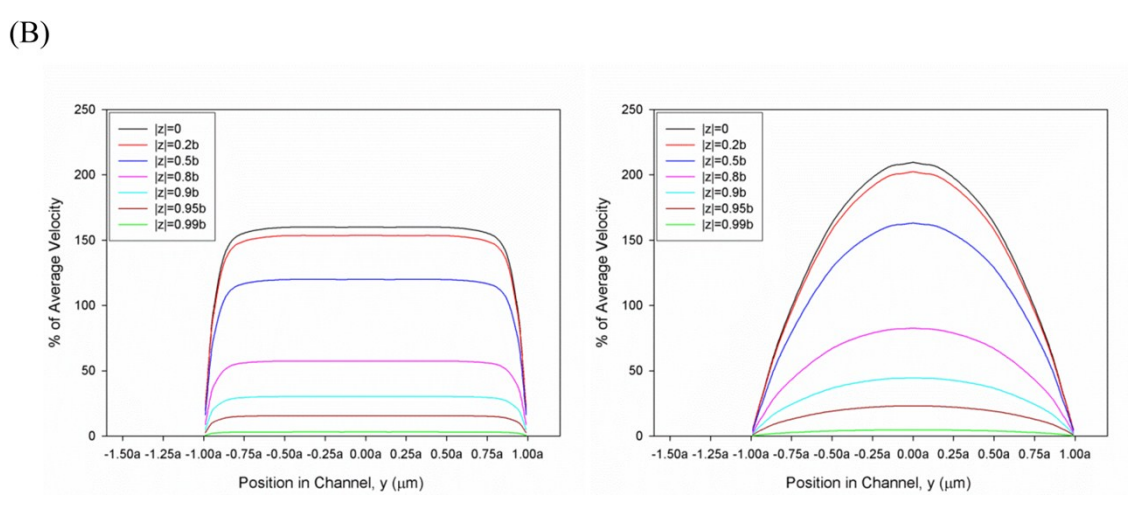
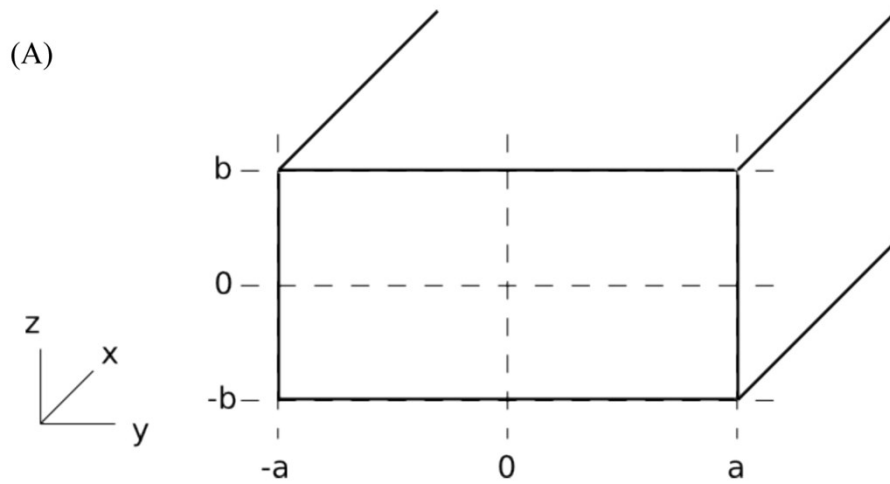


Figure S2: (A). Illustration of channel dimensions as used in Equation S1. The height of the channel is in the z direction, the width in the y direction and the fluid flow is in the x direction. (B) Poiseuille flows for channels of height:width ratios of 1:10 (left) and 1:1 (right). The coloured lines each represent the percentage of the average velocity ($=Q/4ab$ with units of $\text{m}\cdot\text{s}^{-1}$, Q – volumetric flow rate) for different values of z , indicating the height deviation from the centre of the channel in (A). It is clear that the velocity in the centre of most channels will be in the region of 150% to 200% the average velocity, $\frac{Q}{4ab}$.

3. Sample focusing and speed in the detection region

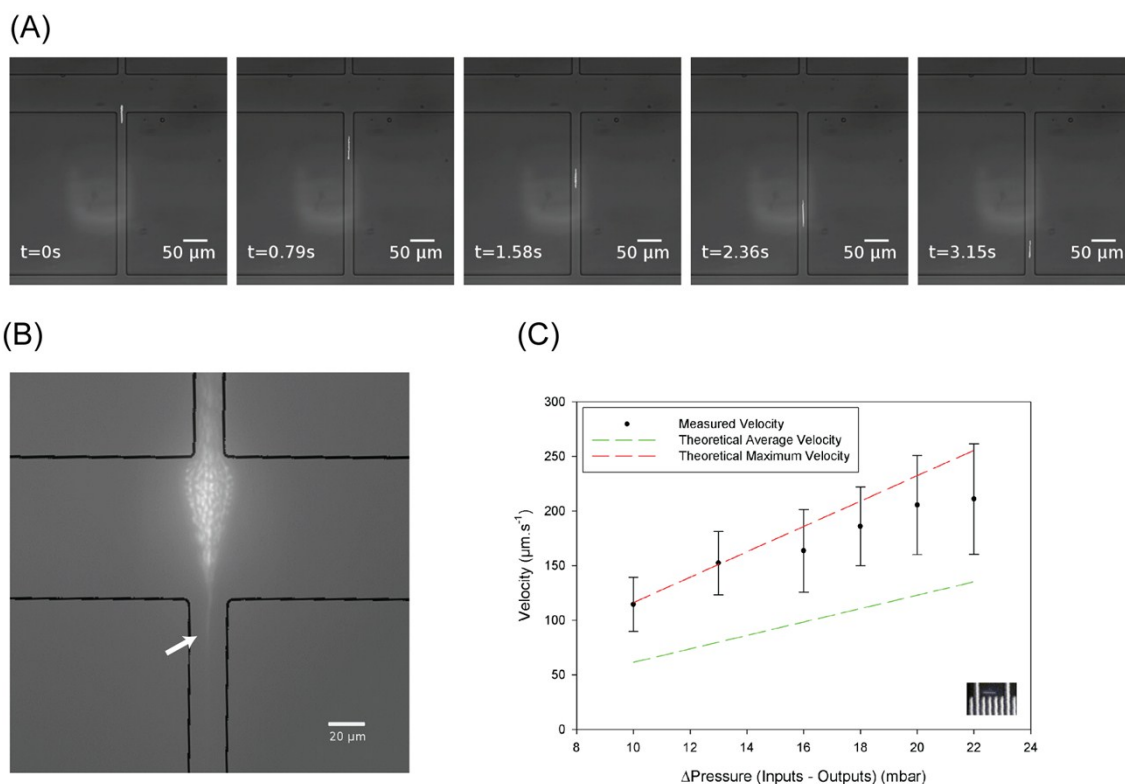


Figure S3. (A) Time-lapse images of a moving fluorescent bead in the detection channel. For easy visualisation, fluorescence images of the bead were superimposed on a bright field image of the channel. Exposure time (t) for each frame is 0.2s. The lengths of the lines (x) left by the beads are proportional to their speed = x/t . (B) Single composite of 1000 exposures. White arrow shows the tight focus of the sample in the detection channel, which has a width less than 3 μm . (C) Measured velocities of fluorescent beads at various pressure differentials. The length of the line shown in (A), is measured against to a scale bar (insert).

4. Evaluation of the collected cells.

To verify the accuracy of sorting after completion of the sorting process and when the microfluidic flow has been halted, Raman spectra of the sorted cells in the collection channel were taken using 100ms acquisition time. These were then used to classify each of the collected cells as either ^{12}C or ^{13}C *Synechocystis* sp. PCC6803, by calculating a correlation coefficient determined by the convolution a given cell's spectrum with each of the reference spectra for ^{12}C and ^{13}C cells. The convolution was performed only in the regions of the ν_1 and ν_2 peaks, i.e. wavenumber between 1089.3 cm^{-1} to 1203.39 cm^{-1} and 1411.0 cm^{-1} to 1551.9 cm^{-1} since this region contains the most distinguishing characteristics of each type of cells. To illustrate this approach, the correlation coefficients of the sorted cells in Figure 7B of the main text are listed in Table S1. A cell was classified as one or other type if the correlation coefficient was >0.75 (see cells No 7 and No10 in Supplementary Figure S4). Whenever the correlation coefficient with both the ^{12}C and ^{13}C *Synechocystis* sp. PCC6803 references was below 0.75, the spectrum was checked to determine whether the best match selected by the software was indeed correct. For example, cell No. 51 in Supplementary Figure S4 was initially classified as a ^{13}C cell and inspection showed this to be the case.

Table S1. Classification of the cells measured in the collection channel.

Cell	¹² C Correlation	¹³ C Correlation	Classi- fication	Cell	¹² C Correlation	¹³ C Correlation	Classi- fication
1	0.62	0.82	13C	41	0.42	0.84	13C
2	0.32	0.72	13C	42	0.37	0.71	13C
3	0.50	0.88	13C	43	0.48	0.69	13C
4	0.34	0.81	13C	44	0.54	0.83	13C
5	0.96	0.43	12C	45	0.97	0.46	12C
6	0.38	0.76	13C	46	0.35	0.88	13C
7	0.40	0.86	13C	47	0.32	0.81	13C
8	0.96	0.46	12C	48	0.43	0.71	13C
9	0.37	0.85	13C	49	0.25	0.48	13C
10	0.97	0.48	12C	50	0.27	0.86	13C
11	0.59	0.73	13C	51	0.35	0.62	13C
12	0.97	0.46	12C	52	0.97	0.48	12C
13	0.46	0.85	13C	53	0.37	0.87	13C
14	0.38	0.77	13C	54	0.28	0.70	13C
15	0.92	0.42	12C	55	0.46	0.73	13C
16	0.40	0.84	13C	56	0.67	0.78	13C
17	0.40	0.82	13C	57	0.96	0.46	12C
18	0.33	0.73	13C	58	0.39	0.84	13C
19	0.97	0.47	12C	59	0.48	0.92	13C
20	0.44	0.79	13C	60	0.32	0.71	13C
21	0.46	0.88	13C	61	0.32	0.75	13C
22	0.97	0.46	12C	62	0.34	0.90	13C
23	0.35	0.86	13C	63	0.44	0.87	13C
24	0.96	0.49	12C	64	0.35	0.83	13C
25	0.40	0.85	13C	65	0.93	0.41	12C
26	0.28	0.69	13C	66	0.25	0.79	13C
27	0.31	0.80	13C	67	0.98	0.45	12C
28	0.97	0.52	12C	68	0.32	0.79	13C
29	0.30	0.74	13C	69	0.48	0.91	13C
30	0.70	0.78	13C	70	0.45	0.84	13C
31	0.40	0.84	13C	71	0.98	0.45	12C
32	0.33	0.81	13C	72	0.42	0.75	13C
33	0.36	0.63	13C	73	0.51	0.77	13C
34	0.39	0.81	13C	74	0.97	0.45	12C
35	0.96	0.49	12C	75	0.33	0.85	13C
36	0.50	0.86	13C	76	0.39	0.84	13C
37	0.90	0.48	12C	77	0.41	0.78	13C
38	0.34	0.80	13C	78	0.95	0.55	12C
39	0.46	0.79	13C	79	0.51	0.82	13C
40	0.21	0.45	13C				
No. of ¹² C <i>Synechocystis</i> sp. PCC6803 cells					19	24.1%	
No. of ¹³ C <i>Synechocystis</i> sp. PCC6803 cells					60	75.9%	

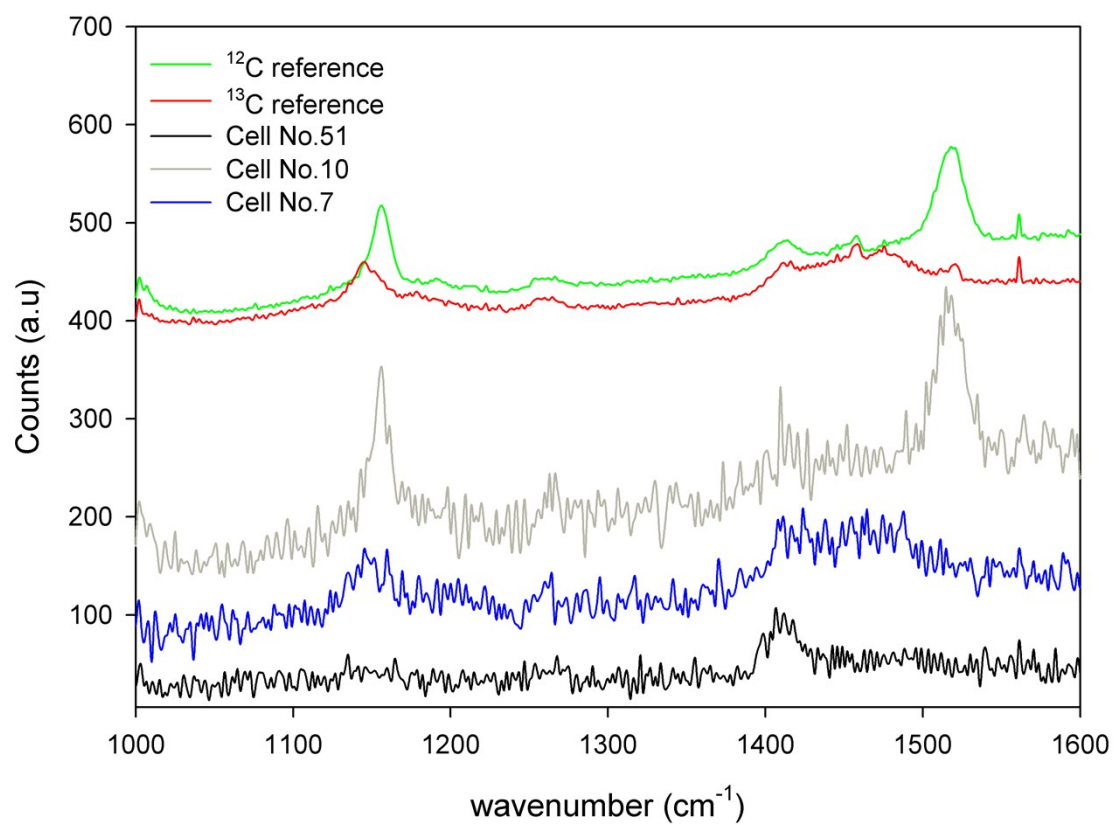


Figure S4. Representative Raman spectra of the sorted cells in the collection channel. The cell IDs correspond to those in Table S1.

Reference:

- [1] White, Frank, and M, *Viscous Fluid Flow*, 2nd ed. New York: McGraw-Hill, 1991.